Autoimmune activation of the GnRH receptor induces insulin resistance in a rat model of polycystic ovary syndrome

Hongliang Li[1*], Gege Zhang[2,3], Yankai Guo[1,2,3], Jielin Deng[1,4], Hayley Fischer[1], LaTasha B Craig[5], David Kem[1], Xichun Yu[1]

Short Title: GnRHR autoantibody-induced insulin resistance in rats

[1]Department of Medicine, Endocrinology section and the Harold Hamm Diabetes Center, The University of Oklahoma Health Sciences Center, Oklahoma City, OK 73104, USA.

[2]Cardiac Pacing and Electrophysiology Department, the First Affiliated Hospital of Xinjiang Medical University, Urumqi, China.

[3]Xinjiang key laboratory of cardiac electrophysiology and remodeling, the First Affiliated Hospital of Xinjiang Medical University, Urumqi, China.

[4]Department of Cardiology, Renmin Hospital of Wuhan University, Wuhan, Hubei, China

[5]Section of Reproductive Endocrinology and Infertility, Department of Obstetrics and Gynecology, The University of Oklahoma Health Sciences Center, Oklahoma City, OK 73104, USA.

Hongliang Li and Gege Zhang contributed equally to this manuscript.

*Corresponding author: Hongliang Li, E-mail address: hongliang-li@ouhsc.edu

Abbreviations:

PCOS: polycystic ovary syndrome

GnRHR-ECL2 AAb: gonadotropin-releasing hormone receptor ECL2 autoantibody

GPCR: G protein coupled receptors

ECL2: extracellular loop 2

LH: luteinizing hormone

T: testosterone

IR: insulin resistance

HPO axis: hypothalamic-pituitary-ovarian axis

Summary:

Polycystic ovary syndrome (PCOS), a metabolic and reproductive disease, is frequently associated with type 2 diabetes. We previously demonstrated that autoantibodies (AAb) directed toward the second extracellular loop (ECL2) of the gonadotropin-releasing hormone receptor (GnRHR) are present in a high percentage of PCOS patients. It is unclear whether GnRHR-AAb can induce peripheral tissue insulin resistance (IR) in animal models. In the present study, we examined the impact of GnRHR-AAb on glucose metabolism, inflammation, and insulin signaling in a recently established autoimmune rat model of PCOS. Sixteen rats were divided into two groups: a GnRHR ECL2 peptide-immunized group, and a control group. Sera GnRHR-AAb, luteinizing hormone (LH), and testosterone were measured by ELISA. All immunized rats produced elevated anti-GnRHR ECL2 antibody titers and higher concentration of testosterone and LH. Intraperitoneal glucose tolerance tests demonstrated higher blood glucose levels in immunized rats at 30 minutes and 60 minutes. A homeostatic model assessment of insulin resistance index was also higher. Furthermore, the mRNA expression levels of insulin signaling genes in peripheral tissue were decreased. The concentration of sera TNF-α, IL-1α, and IL-18 were increased, while IL-4 and IL-10 were inhibited in the immunized group. These data support the likelihood of GnRHR-ECL2 AAbs inducing IR in peripheral tissue. GnRHR-ECL2 AAb may alter the synthesis and pulsatile secretion of LH thus leading to hyperandrogenemia, inflammation, and IR. Our studies provide the realistic expectation of new knowledge regarding the etiology of IR in PCOS as well as a pathway for development of novel effective treatment.

Keywords: autoimmunity, polycystic ovary syndrome, gonadotropin-releasing hormone receptor, inflammatory cytokine, insulin resistance

Introduction

Polycystic ovary syndrome (PCOS) is a common and complex endocrine disorder of women in their reproductive years, with prevalence between 5% and 10% [1]. PCOS is a common endocrinopathy that is associated with hyperandrogenism and an adverse metabolic profile including obesity and insulin resistance [2]. PCOS is characterized by a variable and erratic elevation of luteinizing hormone (LH) of unknown etiology. The hypothalamic/pituitary gonadotropin-releasing hormone (GnRH) system is a key regulator of the reproductive system, triggering the synthesis and release of LH from the pituitary [3]. The etiology of this heterogeneous disorder is unknown and previous attempts to identify an autoimmune pathophysiological target have been unsuccessful. Furthermore, molecular alterations in GnRH or its receptor (GnRHR) have not been associated with causation in PCOS patients.

Our previous studies demonstrated that elevation of an activating autoantibody (AAb) was directed toward the extracellular loop 2 (ECL2) of GnRHR in many subjects with previously diagnosed PCOS. Purified IgG from some of these PCOS subjects with elevated GnRHR-AAb demonstrated a dose-dependent effect on GnRHR activation in GnRHR-transfected cells; and this in vitro activity was suppressed by the GnRHR antagonist-Cetrorelix [4]. This important and novel discovery and its potential involvement in the receptor control of LH release raises the possibility that PCOS constitutes an autoimmune disease.

Insulin resistance and impaired glucose tolerance are present in a large percentage (ranging from 44%-70%) of women with PCOS [5]. Insulin resistance is a key contributor to metabolic disturbance and is a driver in the pathogenesis of PCOS. Previous studies reported that all three primary energy storage tissues, liver, white adipose tissue(WAT), and

skeletal muscle, showed impaired insulin signaling pathway in PCOS models[6-8]. How insulin dysregulation occurs in this syndrome is not entirely known. Multiple studies showed associations between insulin resistance and hyperandrogenism in human[9] and animal models[10].

Women with PCOS may have chronic low level inflammation [11]. Adiposity may play a central role in generating and maintaining the syndrome [12]. Visceral adipose tissue is strongly linked to both inflammation and insulin resistance through produces various pro-inflammatory cytokines. Rui et al[13] reported that TNF-α possibly acting as the triggering cytokine in these events. Recent study showed that excess androgens cause adipocyte hypertrophy and increase inflammation, which is related to insulin resistance[14]. However, it is still unclear whether androgen excess in PCOS promotes a state of inflammation.

In this study, we first established an autoimmune rat model with an immunological GnRHR ECL2 peptide to further detect GnRHR-AAb activity and androgen concentrations. We also evaluated the effects of GnRHR-AAb on insulin signaling and inflammatory status. The results showed that GnRHR-AAb induces insulin resistance associated with excess androgen and inflammatory cytokines.

Materials and methods

Animals and experimental protocol

Sixteen rats were divided into two groups: an immune group (PCOS group) and a control group. Eight rats in the immune group (average weight 150-175g) were immunized with 1mg/Kg of GnRHR-ECL2 peptide in 200μl complete Freund's adjuvant. The rats were boosted with the same peptide with incomplete Freund's adjuvant at 4, 8, 12, and 16 weeks. Sera were obtained from all rats for antibody detection (Figure 1). All animal experimental procedures were reviewed and approved by the Institutional Animal Care Committee

(IACUC300837) and performed according to American Veterinary Medical Association criteria.

Enzyme-linked immunosorbent assay

Antibody titers in sera were determined by ELISA. Briefly, microtiter plates were coated with GnRHR ECL2 target peptide at 10 µg/ml in coating buffer. Sera was diluted in a series of concentrations from 1:20,000 to 1:2,560,000 in diluent buffer. Alkaline phosphatase-conjugated affinipure goat anti-rat IgG and alkaline phosphatase substrate were used in following detection. Titers were determined as the highest dilution with an OD value of 0.10 at 60 minutes.

LH (ENZ-KIT 107, Enzo Life Sciences, Farmingdale, NY, USA) and free testosterone (T) (ADI-900-065, Enzo Life Sciences, Farmingdale, NY, USA) concentrations were detected with ELISA kits following the manufacturer's protocol. Sera samples were diluted 1:50 with a standard diluent prepared before testing. Plates were coated with goat anti-mouse IgG and mouse monoclonal LH or free T antibodies for their appropriate assays were added to the plate after standards and samples. Then alkaline phosphatase conjugate and p-nitrophenyl phosphate were used to determine hormone concentration. OD value at 405 nm was read after stop solution was added.

Cell-based GnRHR assay

Sera activation of GnRHR in GnRHR-NFAT-bla CHO-K1 cells were assessed using the GeneBLAzer FRET-based β-lactamase reporter assay (Invitrogen) according to manufacturer's instructions. Briefly, cells were plated in 384-well plates and incubated overnight. The individual sera samples and positive and negative controls were then added and incubated for 4 hours. The β-lactamase substrate CCF4-AM (LiveBLAzer-FRET B/G Loading Kit, Invitrogen, Carlsbad, CA, USA) was then added and incubated at room

temperature for 2 hours in the dark. The plates were read using a fluorescence microplate reader (BioTek Synergy 2 Multi-Detection Microplate Reader). All samples were assayed in triplicate. Data were expressed as the ratio of the emissions 460/530 nm (blue/green) after subtraction of the background values.

Fasting blood glucose, body weight, intraperitoneal glucose tolerance tests (IPGTT)

Rat weights were measured using an electronic scale at 0, 4, 8, 12, 16, and 20 weeks. The IPGTT was performed at 18 weeks. For this procedure each rat was fasted overnight and deprived of water. Then 5 µl of blood (one drop) from the back leg vein was transferred directly onto a glucose indicator strip for assay of blood glucose with a glucometer (ONETOUCH$^{@}$Verio Flex, Lifescan, USA). The rats were given an intraperitoneal injection of glucose (2 g/kg) with a 24 G needle. Blood samples were obtained before the glucose injection and at 15, 30, 60, and 120 min. The rats were returned to their cage and monitored visually between each of these time points. Related area under curve (AUC), describing blood glucose levels in each rat after glucose loading, was calculated[15].

Insulin sensitivity evaluation by HOMA-IR

By the end of week 20, a venous blood sample was drawn from each individual rat after 12 hours of fasting. The sera was separated from the collected blood samples by centrifugation for 10 min at 2000 rpm and stored at -80°C. The levels of insulin were analyzed by ELISA (ERINS, Thermo Fisher Scientific, Waltham, MA, USA) per the manufacturer's instructions. The value of homeostatic model assessment of insulin resistance (HOMA-IR) was calculated as the following: HOMA-IR = (fasting glucose × fasting insulin)/22.5. This value was inversely proportional to insulin sensitivity [16, 17].

In vivo insulin administration

At 20 weeks, the control and PCOS rats were fasted over night and administered 0.5U/kg body weight(BW) insulin via intraperitoneal (ip) injection (Eli Lilly, Indianapolis, IN) or saline. Ten minutes after ip injection, the mice were euthanized with CO2, and liver tissues, WAT, pituitaries, and ovaries were extracted.

RT-PCR analysis

Liver tissues, WAT, and skeletal muscle tissues from fed rats were harvested. RNA was extracted by lysing tissue (≤ 5 mg) in 300µl of TRI reagent (732-6890, Bio Rad, Hercules, California, USA) and homogenized. In order to remove particulate debris, homogenized tissue was centrifuged and the supernatant transferred into an RNase-free tube. RNA purification included application of prepared samples in TRI reagent directly to the Zymo-Spin IC column and subsequent spinning, washing, and elution of the RNA. cDNA was synthesized with a reaction mix [4 µl iScript reverse transcription supermix (1708841, Bio Rad, Hercules, California, USA), 2µl RNA, and 14 µl nuclease-free water] in a thermal cycle (5 min at 25℃, 20 min at 46℃, and 1 min at 95℃). Finally, RT-PCR was done with the reaction mix [10µl iTaq SYBR Green supermix (1725124, Bio Rad, Hercules, California, USA), 1µl of each forward and reverse primers 1µl cDNA, and 7µl nuclease-free water] in a thermal cycle. During the experiment, an iCycler iQ5 Q-PCR machine (Bio-Rad, Hercules, California, USA) was used. All primers are indicated in Table 1.

Western blot analysis

Liver tissues, WAT and skeletal muscle tissue from fed and overnight fasted rats were harvested. Small tissue pieces (≤ 5 mg) were homogenized in 1ml RIPA lysis buffer. The protein concentration was measured by a spectrophotometer (ND-1000, NanoDrop, Marshall Scientific, Boston, USA), and then all samples were balanced to the same concentration of protein. Mixed with loading buffer, samples were separated by SDS-PAGE

(Thermo Scientific, Waltham, MA, USA) gel and transferred to a nitrocellulose membrane. TBS-T containing 5% BSA was used to block the membrane before adding primary mouse anti-rat antibodies (p-AKT) (sc-293125, Santa Cruz Biotechnology, Texas, Dallas, USA) @ 1:200 incubation. Membranes were washed 3 times with TBS-T and secondary anti-mouse antibody (sc-516102, Santa Cruz Biotechnology, Texas, Dallas, USA) was diluted 1:1000 and used for incubation. Protein bands were detected in a chemiluminescent detection mix (GE Healthcare) and detected with an imaging system (Image J).

Immunofluorescence detection of IRS-1 and PI3K

Rats' tissues, including liver tissues, WAT and skeletal muscle, were fixed in paraffin and cut into slices. Hydrogen peroxide blockade was added to cover sections and then antigen retrieval was done in citrate buffer (pH 6). After protein blocking for 10 min, mouse anti-rat antibodies (IRS-1, sc-8038; PI3k sc-293172, Santa Cruz Biotechnology, Texas, Dallas, USA) were applied and incubated overnight at 4 ℃. The sections sequentially were incubated with secondary Alexa Fluor 555-conjugated goat polyclonal anti-mouse IgG (A32727; Thermo Fisher Scientific, Miami, OK, USA) and secondary Alexa Fluor 488-conjugated goat polyclonal anti-mouse IgG (A32723; Thermo Fisher Scientific, Miami, OK, USA), respectively. Hematoxylin was added to sections before they were placed in 100% alcohol, xylene, and mounted with cover slips. The images were recorded using a confocal laser scanning microscope (Leica TCS SP5, Germany).

Analysis of inflammatory biomarkers

The levels of inflammatory markers tumor necrosis factor (TNF-α), interleukin (IL)-1α, interleukin (IL)-4, interleukin (IL)-10, and interleukin (IL)-18 were measured in sera from all the rats. This was done using Bio-plex Pro™ magnetic bead-based assays (Bio-Rad, Hercules, USA) on the Bio-plex® platform (Bio-Rad), according to the manufacturer's

instruction. Following previous optimization, samples were evaluated undiluted, in a blinded manner. Bio-Plex Manager™ software, version 6.0 was used for bead acquisition and analysis.

Statistical analysis

Data are expressed as mean ± standard error of the man (SEM). Two-tailed students' tests were used for comparison between two groups, and repeated-measures ANOVA tests were used for comparison among three. Values of p <0.05 were deemed statistically significant.

Results

A PCOS rat's model with GnRHR-AAb of high titer and activity

Immunized for 20 weeks, the GnRHR-AAb titer (Figure 2A) and GnRHR-AAb activity (Figure 2B) was tested with ELISA. Sera of PCOS and control rats were diluted to 1: 256,000 and exposed to the coated GnRH-ECL2 peptide. The strength of reactions were expressed with OD value at the same dilution. Results showed that the OD values of PCOS rats were significantly higher than that of control rats (p<0.01). The GnRHR-AAb activity for the PCOS groups was significantly greater than the controls (p<0.01).

Elevated GnRHR-AAb levels increase LH and testosterone concentrations in PCOS rats

The concentration of LH (Figure 3A) and T (Figure 3B) in sera of both groups were detected with ELISA kits. Sera from rats at 16 weeks was used and diluted to 1:50. After calculated with standard curves, PCOS rats displayed higher concentrations of LH and T compared with control rats (p<0.05).

Metabolic changes after elevated GnRHR-AAb levels in PCOS rats

During the experiment, all rats were measured for body weight (Figure 4A) and fasting blood glucose levels (Figure 4B). There was no significant difference between the PCOS rats and

the control group (p>0.05). However, as the experiment proceeded, we observed that the fasting blood insulin levels in the PCOS rats gradually increased compared with the control group (p<0.01) (Figure 4C). Two weeks ahead of the terminal study, all rats underwent an IPGTT study. After glucose was injected, blood glucose levels were recorded and are shown in Figure 4D. Glucose levels in both groups were low at baseline and elevated rapidly at 15 min. There was a minor decrease at 30 min before an obvious one at 60 min. At 120 min, the glucose levels returned to baseline. However, it was found that the glucose levels of PCOS rats at 30 and 60 min were higher than those of control rats with an apparent slower clearance of blood glucose. The incremental area under the two-hour blood glucose response curves was calculated and shown for the two groups in Figure 4E. The AUC of PCOS group was higher than that of the control group (p<0.01). The calculated HOMA-IR index of reactive insulin sensitivity was also significantly increased in the PCOS rats group compared to the controls animals (p<0.01) (Figure 4F).

GnRHR-AAb decreases expression of insulin signaling in liver, WAT, and skeletal muscle

mRNA expression of insulin signaling genes were examined by RT-PCR. Representative genes of insulin signaling and glucose transport were included in the PCR and included hepatic (PI3K, AKT, GLUT-2, Figure 5A), WAT (IR, IRS-1, AKT, GLUT-4, Figure 5B), and skeletal muscle (AKT, GLUT-4, Figure 5C). These were significantly decreased in immunized rats compared with the controls (p<0.05).

Western blot analysis demonstrated representative bands and quantified the influence of 20 weeks GnRH immunization of rats on protein expression levels in different peripheral tissue as shown in Figure 6 (A represents liver tissue, B represents WAT, and C represents

skeletal tissue). The expression of p-AKT decreased significantly in the PCOS group compared with control group ($p<0.05$).

Protein expression of insulin signaling was tested with immunofluorescence staining in serveral tissues. Representative images of IF staining are shown in Figure 7A and target proteins were stained red (IRS-1) and green (PI3K). Compared with non-immunized controls, expression of IRS-1 (Figure 7B) and PI3K (Figure 7C) were lower in the PCOS group ($p<0.01$).

Markers of chronic inflammation were increased after elevated GnRHR-AAb levels

The effects of GnRHR autoantibody on TNF-α, IL-1α, IL-4, IL-10 and IL-18 are illustrated in Figure 8. The concentration of proinflammatory cytokines (TNF-α, IL-1α, IL-18) were significantly increased in the sera of the GnRHR immunized rats compared with the control rats (Figure 8A). PCOS rats also demonstrated significantly reduced anti-proinflammatory proteins (IL-4, IL-10) when compared with normal control rats (Figure 8B).

Discussion

In the current study, we induced an autoimmune rat model using a specific synthetic GnRHR ECL2 peptide. GnRHR-AAb activity, LH and T concentrations were elevated in this rat model compatible with that observed in humans with PCOS. The increased GnRHR-ECL2 AAb and T appear to induce insulin resistance by inhibiting IRS-1-PI3K-Akt signaling and producing reciprocal changes in certain inflammatory cytokines. Our results support the notion that antibody activation of GRHR and the subsequent increase in androgens and chronic inflammation may be important mechanisms associated with PCOS and insulin resistance (Figure 9). In this experiment we found that the increased LH and T secretion in immunized rats indicates that GnRHR antibody could specifically bind to and activate

GnRHR to stimulate the synthesis and secretion of these hormones characteristically observed in PCOS .

Although we did not directly assess insulin sensitivity, we measured surrogate markers of insulin sensitivity such as fasting serum insulin, fasting blood glucose, and the HOMA-IR index (which reflects the glucose-insulin relationship). Our results demonstrated that the fasting blood glucose in GnRHR immunized rats did not change; however, the blood glucose level at 30 min and 60 min in IPGTT test was increased and the AUC blood glucose concentration during IPGTT was also increased. The insulin levels were significantly increased and the HOMA-IR index estimating the peripheral insulin resistance was significantly higher in the PCOS rats than in the control group, suggesting that PCOS rats developed insulin resistance. Currently, PCOS animal models are mainly divided into two types: androgen and gene induction models [18]. The androgens currently used to induce PCOS in mice are mainly dihydrotestosterone (DHT) [19, 20], dehydroepiandrosterone (DHEA)[21] and T[22]. Both prenatal [19] and prepubertal [20] DHT administration causes metabolic alterations, such as increased obesity, altered adipokine levels, and glucose intolerance. Treatment with DHEA induced an increase in body weight, and also increased fasting insulin and glucose levels [21]. Testosterone-induced mouse models[22] cannot be fully excluded as their metabolic phenotype (including conversion to dihyrotestosterone) has been less extensively studied. Genetic models are useful in understanding the etiology of PCOS, but they do not fully replicate the phenotype of PCOS [23].

The mechanistic interaction between GnRHR-AAb and the insulin signaling pathway is still unclear. Andrisse et al[10] established a PCOS mouse model by administration of low dose dihydrotestosterone (DHT) and found that energy storage tissues displayed differential effects on the insulin-signaling pathway. WAT and liver displayed lower mRNA

and protein expression of insulin signaling intermediates while skeletal muscles exhibited normal levels. We provide evidence that experimentally induced elevation of GnRHR-ECL2 AAb in rats decreases the expression of insulin signaling mRNA and proteins in WAT and liver tissue. However, we also observed that an insulin signaling pathway was down-regulated in skeletal muscles. We hypothesize that GnRHR-AAb induces LH secretion resulting in an increase in the synthesis and secretion of androgen and thus interrupting insulin signaling pathways in peripheral tissues. This supports the concept that GnRHR-ECL2 AAb induced hyperandrogenemia may be the key to induction of insulin resistance.

We observed a reciprocal rise in the inflammatory response in the immunized group. Compared with the control group, the level of pro-inflammatory cytokines (TNF-α, IL-1α, and IL-18) were significantly increased in the immunized group, while the level of anti-inflammatory cytokines (IL-4 and IL-10) was significantly decreased. Our findings are consistent with previous studies demonstrating increased proinflammatory and decreased anti-inflammatory cytokines in PCOS patients[24-31]. Our experiment indicates that GnRHR-ECL2 AAb may lead to an imbalance between pro- and anti-inflammatory cytokines and further induce peripheral insulin resistance.

Previous studies have implied that androgen, adipose tissue, and inflammatory factors are closely linked[21, 32]. It is still unclear whether androgen excess in PCOS promotes a state of inflammation. Androgens cause adipocyte hypertrophy and this could explain their involvement in the development of chronic low-grade inflammation [14]. Our data highlights the importance of GnRHR-ECL2 AAb in triggering inflammation and insulin resistance by secondarily stimulating-androgen production.

In summary, we have provided evidence that GnRHR-ECL2 AAb induces insulin resistance in energy storage tissue and peripheral tissue. GnRHR-ECL2 specific AAb may

alter the synthesis and pulsatile secretion of LH, leading to hyperandrogenemia, insulin resistance, and metabolic abnormalities. Our studies provide the realistic expectation of new knowledge regarding the etiology of insulin resistance in PCOS as well as a pathway for development of novel effective treatment. This rat model, with our previously reported data demonstrating the presence of GnRHR-ECL2 activating autoantibodies in humans, fulfills Witebsky's criteria for an autoimmune basis for PCOS [33].

Acknowledgements

This study was supported by the grants from Oklahoma Center for Advancement of Science and Technology and an individual grant from Will and Helen Webster.

Disclosures

The authors declare no conflicts of interest.

Author contributions

H. L. conceived the study idea, designed the experiments, performed experiments, analyzed the results, reviewed and edited the manuscript; G. Z. performed experiments, analyzed the results, drafted and wrote the manuscript; Y. G. and J. D. performed experiments; H. F. supervised the study and edited the manuscript; L. C, D. K., and X. Y. supervised and administered the project, reviewed, and edited the manuscript.

References

1. Azziz R, Woods KS, Reyna R, Key TJ, Knochenhauer ES, Yildiz BO. The prevalence and features of the polycystic ovary syndrome in an unselected population. The Journal of Clinical Endocrinology & Metabolism 2004; 89:2745-49.
2. Bremer AA. Polycystic ovary syndrome in the pediatric population. Metabolic syndrome and related disorders 2010; 8:375-94.
3. Christensen A, Bentley G, Cabrera R, Ortega H, Perfito N, Wu T, Micevych P. Hormonal regulation of female reproduction. Hormone and metabolic research 2012; 44:587-91.
4. Craig LB, Reynolds AC, Burks HR, Li H, Yu X, Aston CE, Elkosseifi M, Kem DC. Stimulating autoantibodies directed to the gonadotropin releasing hormone receptor are sensitive and specific for polycystic ovary syndrome. Fertility and sterility 2017; 108:e259.
5. Macut D, Bjekic-Macut J, Rahelic D, Doknic M. Insulin and the polycystic ovary syndrome. Diabetes Res Clin Pract 2017; 130:163-70.
6. Andrisse S, Childress S, Ma Y, Billings K, Chen Y, Xue P, Stewart A, Sonko ML, Wolfe A, Wu S. Low-dose dihydrotestosterone drives metabolic dysfunction via cytosolic and nuclear hepatic androgen receptor mechanisms. Endocrinology 2017; 158:531-44.
7. Corbould A, Dunaif A. The adipose cell lineage is not intrinsically insulin resistant in polycystic ovary syndrome. Metabolism 2007; 56:716-22.
8. Højlund K, Glintborg D, Andersen NR, Birk JB, Treebak JT, Frøsig C, Beck-Nielsen H, Wojtaszewski JF. Impaired insulin-stimulated phosphorylation of Akt and AS160

in skeletal muscle of women with polycystic ovary syndrome is reversed by pioglitazone treatment. Diabetes 2008; 57:357-66.

9. Polderman KH, Gooren L, Asscheman H, Bakker A, Heine RJ. Induction of insulin resistance by androgens and estrogens. The Journal of Clinical Endocrinology & Metabolism 1994; 79:265-71.

10. Andrisse S, Billings K, Xue P, Wu S. Insulin signaling displayed a differential tissue-specific response to low-dose dihydrotestosterone in female mice. American Journal of Physiology-Endocrinology and Metabolism 2018; 314:E353-E65.

11. González F. Inflammation in polycystic ovary syndrome: underpinning of insulin resistance and ovarian dysfunction. Steroids 2012; 77:300-05.

12. Puder JJ, Varga S, Kraenzlin M, De Geyter C, Keller U, Müller B. Central fat excess in polycystic ovary syndrome: relation to low-grade inflammation and insulin resistance. The Journal of Clinical Endocrinology & Metabolism 2005; 90:6014-21.

13. Rui L, Aguirre V, Kim JK, Shulman GI, Lee A, Corbould A, Dunaif A, White MF. Insulin/IGF-1 and TNF-α stimulate phosphorylation of IRS-1 at inhibitory Ser 307 via distinct pathways. The Journal of clinical investigation 2001; 107:181-89.

14. Spritzer PM, Lecke SB, Satler F, Morsch DM. Adipose tissue dysfunction, adipokines, and low-grade chronic inflammation in polycystic ovary syndrome. Reproduction 2015; 149:R219-R27.

15. Jørgensen MS, Tornqvist KS, Hvid H. Calculation of glucose dose for intraperitoneal glucose tolerance tests in lean and obese mice. Journal of the American Association for Laboratory Animal Science 2017; 56:95-97.

16. Matthews D, Hosker J, Rudenski A, Naylor B, Treacher D, Turner R. Homeostasis model assessment: insulin resistance and β-cell function from fasting plasma glucose and insulin concentrations in man. Diabetologia 1985; 28:412-19.

17. Polak K, Czyzyk A, Simoncini T, Meczekalski B. New markers of insulin resistance in polycystic ovary syndrome. Journal of endocrinological investigation 2017; 40:1-8.

18. van Houten EL, Visser JA. Mouse models to study polycystic ovary syndrome: a possible link between metabolism and ovarian function? Reprod Biol 2014; 14:32-43.

19. Roland AV, Nunemaker CS, Keller SR, Moenter SM. Prenatal androgen exposure programs metabolic dysfunction in female mice. The Journal of endocrinology 2010; 207:213.

20. van Houten ELA, Kramer P, McLuskey A, Karels B, Themmen AP, Visser JA. Reproductive and metabolic phenotype of a mouse model of PCOS. Endocrinology 2012; 153:2861-69.

21. Solano ME, Sander VA, Ho H, Motta AB, Arck PC. Systemic inflammation, cellular influx and up-regulation of ovarian VCAM-1 expression in a mouse model of polycystic ovary syndrome (PCOS). Journal of reproductive immunology 2011; 92:33-44.

22. Liu X, Andoh K, Mizunuma H, Kamijo T, Kikuchi N, Yamada K, Ibuki Y. Effects of recombinant human FSH (rhFSH), urinary purified FSH (uFSH), and hMG on

small preantral follicles and tertiary follicles from normal adult and androgen-sterilized female mice. Fertility and sterility 2000; 73:372-80.

23. van Houten ELA, Visser JA. Mouse models to study polycystic ovary syndrome: a possible link between metabolism and ovarian function? Reproductive biology 2014; 14:32-43.

24. Duleba AJ, Dokras A. Is PCOS an inflammatory process? Fertility and sterility 2012; 97:7-12.

25. Makedos A, Goulis D, Arvanitidou M, Mintziori G, Papanikolaou A, Makedou A, Panidis D. Increased serum C-reactive protein levels in normal weight women with polycystic ovary syndrome. Hippokratia 2011; 15:323.

26. Amato G, Conte M, Mazziotti G, Lalli E, Vitolo G, Tucker AT, Bellastella A, Carella C, Izzo A. Serum and follicular fluid cytokines in polycystic ovary syndrome during stimulated cycles. Obstetrics & Gynecology 2003; 101:1177-82.

27. Okamura H, Tsutsui H, Kashiwamura S-I, Yoshimoto T, Nakanishi K. Interleukin-18: a novel cytokine that augments both innate and acquired immunityAdvances in immunology: Elsevier, 1998:281-312.

28. Stephens J, Butts M, Pekala P. Regulation of transcription factor mRNA accumulation during 3T3-L1 preadipocyte differentiation by tumour necrosis factor-α. Journal of molecular endocrinology 1992; 9:61-72.

29. Heinrich PC, Castell JV, Andus T. Interleukin-6 and the acute phase response. Biochemical journal 1990; 265:621.

30. Yang Y, Qiao J, Li R, Li M-Z. Is interleukin-18 associated with polycystic ovary syndrome? Reproductive Biology and Endocrinology 2011; 9:7.

31. Vural P, Değirmencioğlu S, Saral NY, Akgül C. Tumor necrosis factor α (− 308), interleukin-6 (− 174) and interleukin-10 (− 1082) gene polymorphisms in polycystic ovary syndrome. European Journal of Obstetrics & Gynecology and Reproductive Biology 2010; 150:61-65.

32. Eisner JR, Dumesic DA, Kemnitz JW, Colman RJ, Abbott DH. Increased adiposity in female rhesus monkeys exposed to androgen excess during early gestation. Obesity research 2003; 11:279-86.

33. Rose NR, Bona C. Defining criteria for autoimmune diseases (Witebsky's postulates revisited). Immunology today 1993; 14:426-30.

Figure legend:

Figure 1. Immunization design of protocol performed on the rats. Sixteen rats were divided into two groups: immune group and control group. All rats in the immunized group were immunized with GnRHR ECL2 peptide at the beginning of experiment and they were boosted with peptide every 4 weeks. Rats were killed at week 20 in which blood and tissue samples were collected for subsequent studies.

Figure 2. GnRHR antibody titer and GnRHR activity tested by ELISA of immune rats after 8, 16, and 20-week immunization and control rats. Immune rats developed high titer of GnRHR antibody after being immunized. ** $p<0.01$ vs. control.

Figure 3. Concentration of LH (A) and testosterone (B) detected by ELISA in sera. Immune rats were found with higher concentration of LH and testosterone compared with control ones after 16 weeks immunization. * $p<0.05$ vs. control.

Figure 4. Insulin resistance occurs after immunization. Rats body weight change (A), Fasting blood glucose (B), Insulin concentration (C), Intraperitoneal glucose tolerance test (D), Related area under curve (AUC) (E), and HOMA-IR (F). During the experiment, there was no significant difference in rat's body weight changes or fasting blood glucose level between the experimental group and the control group. Insulin concentrations increased significantly compared with control group. Rats were injected with 2g/kg glucose at baseline (BS) and blood glucose level was tested at 15, 30, 60, and 120 min. Blood glucose levels of immune rats were higher at 30 and 60 min than those of control rats. The incremental area under the two-hour blood glucose response curve was compared and immune rats displayed larger of AUC. HOMA-IR levels of immune rats were higher than those of control rats. ** $p<0.01$ vs. control.

Figure 5. Insulin signaling pathway genes expression detected by RT-PCR in liver tissue (A), white adipose tissue (WAT, B) and skeletal muscle tissue (C). The mRNA expression of both insulin signaling and glucose transporter genes in the liver (PI3K, AKT, GLUT-2), white adipose tissue (IR, IRS-1, AKT, GLUT-4), and skeletal muscle (AKT, GLUT-4) were significantly lowered by GnRHR antibodies in immune rats compared with the controls. *p<0.05 vs. control.

Figure 6. Representative images of western blot of p-AKT and β-Actin protein levels in liver tissue (A), WAT (B), and skeletal muscle (C). Immune rats displayed lower protein levels of p-AKT after 20-week immunization of GnRHR ECL2 peptide. * p<0.05 vs. control.

Figure 7. Representative images (Figure 7A) of immunofluorescence staining in liver tissue, WAT, and skeletal muscle, and target proteins were stained red (IRS-1) and green (PI3K). Immune rats expressed decreased protein level of IRS-1 (Figure 7B) and PI3K (Figure 7C) in the liver, WAT, and skeletal muscle compared with control rats. * p<0.05 vs. normal control. ** p<0.01 vs. normal control.

Figure 8. Effects of GnRHR autoantibody on levels of TNF-α, IL-1α, IL-4, IL-10, and IL-18 in normal and PCOS rats. The concentration of pro-inflammatory cytokines (TNF-α, IL-1α, IL-18) were significantly increased in the sera of GnRHR immunized rats when compared with the control rats (Figure 8A). PCOS rats displayed significantly reduced anti-proinflammatory proteins (IL-4, IL-10) when compared with normal control rats (Figure 8B). * p<0.05 vs. normal control. ** p<0.01 vs. normal control.

Figure 9. Representative images of the proposed pathophysiological mechanisms of GnRHR-ECL2 AAb, hyperandrogenemia, inflammation, and insulin resistance in PCOS. GnRHR-ECL2 AAb can promote the release of GnRH from the hypothalamus and release of LH from the pituitary gland. The presence of high concentration of testosterone can be

detected in the blood and elevated sera testosterone levels lead to the rebalancing of inflammatory factors in this disorder and thereby induce insulin resistance.

Figure 1

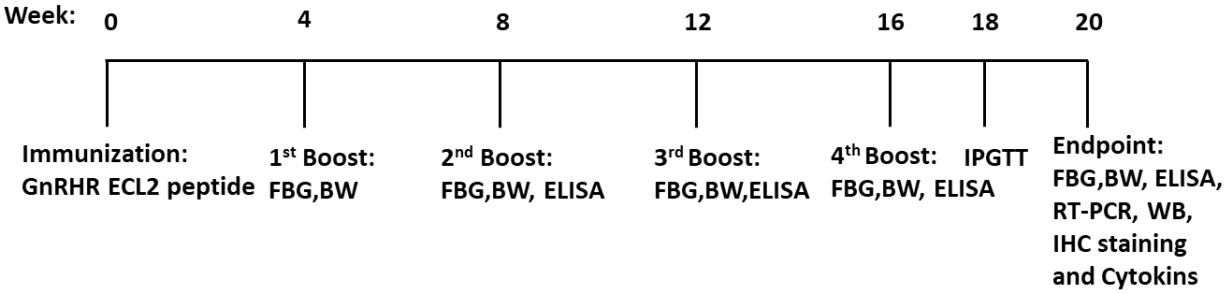

Figure 2

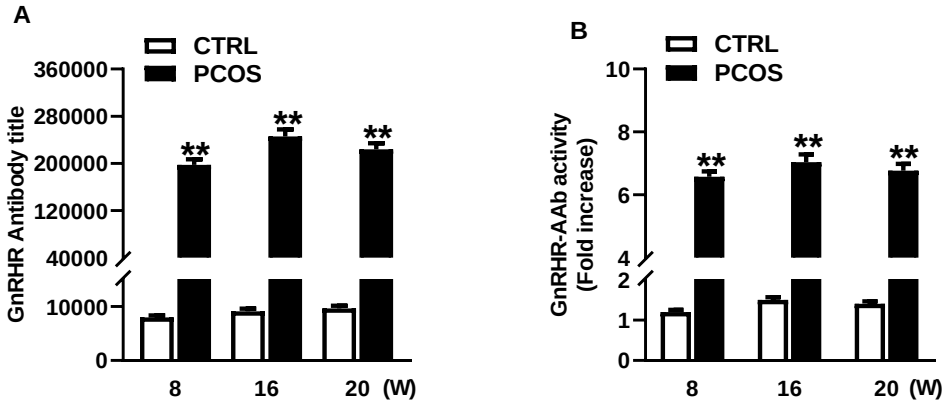

Figure 3

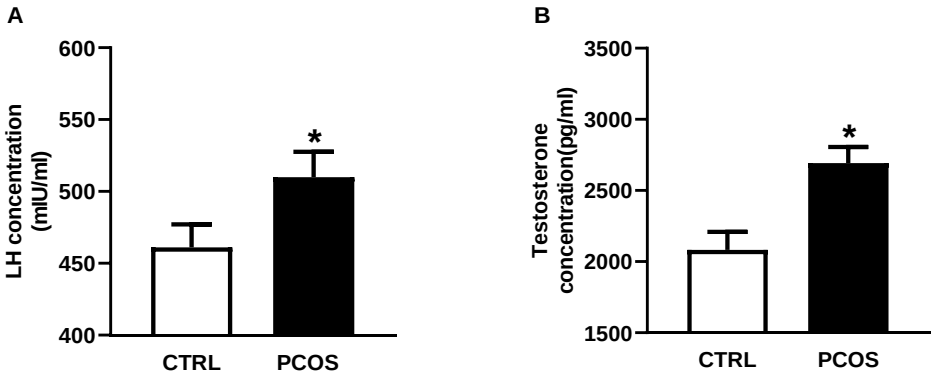

Figure 4

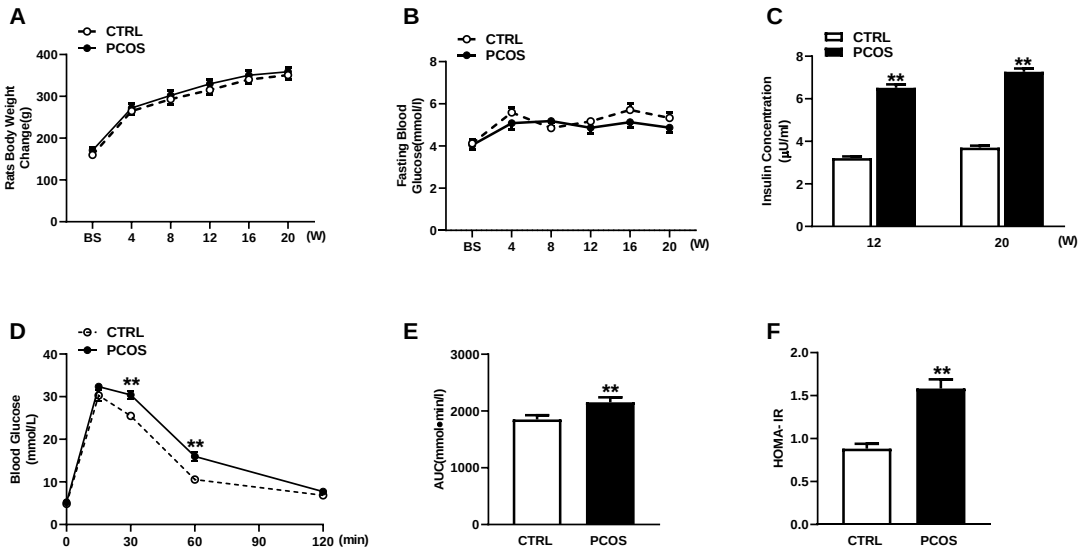

Figure 5

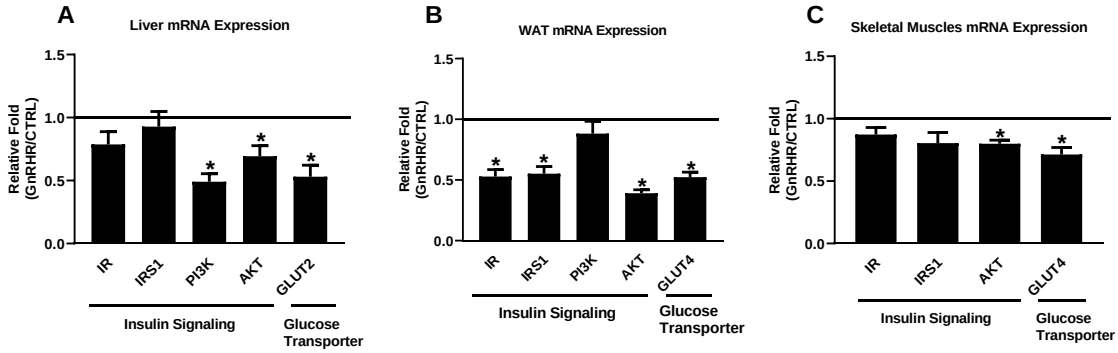

Figure 6

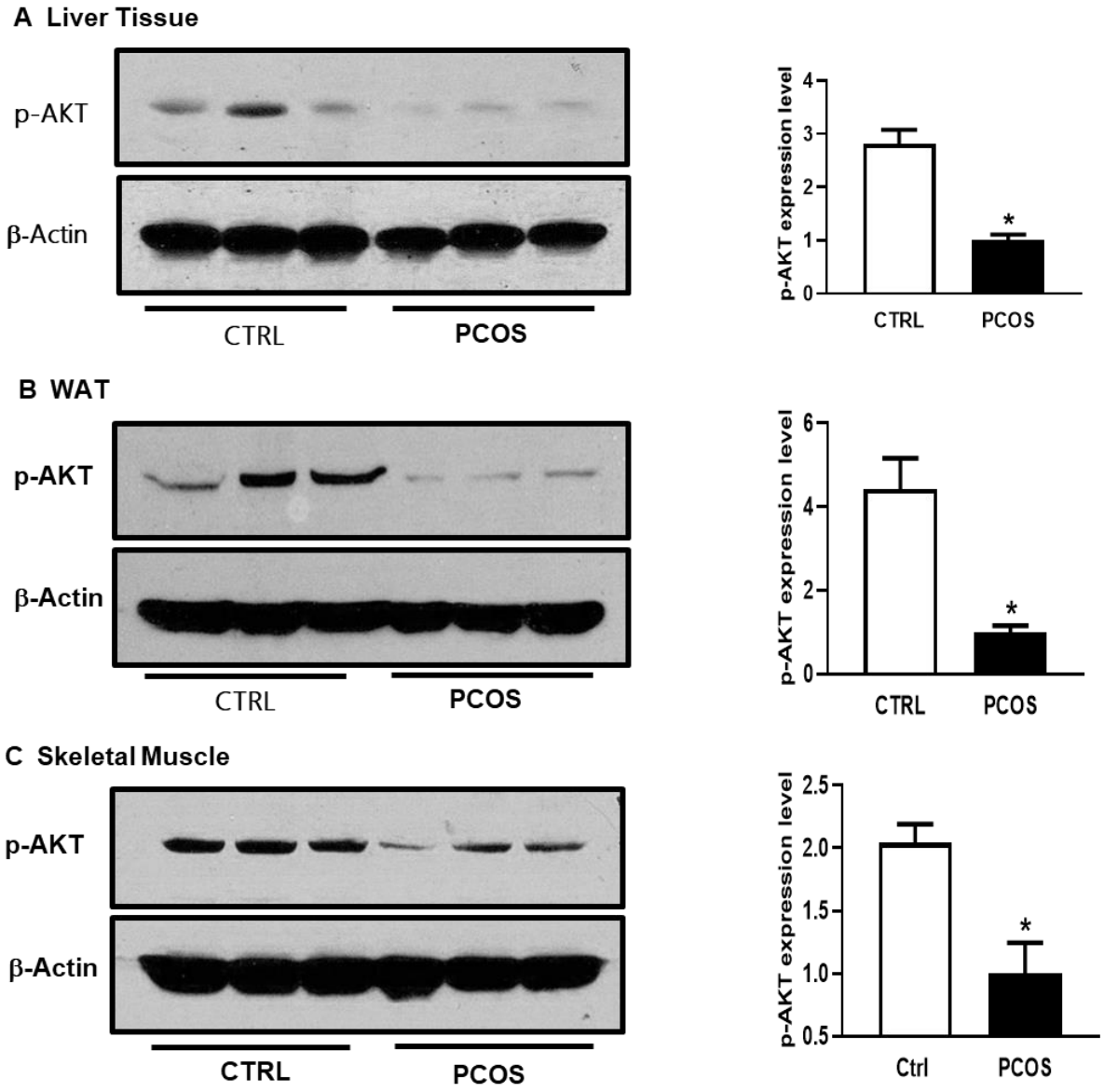
A Liver Tissue
p-AKT
β-Actin
CTRL
PCOS
p-AKT expression level
4
3
2
1
0
*
CTRL
PCOS
B WAT
p-AKT
β-Actin
CTRL
PCOS
p-AKT expression level
6
4
2
0
*
CTRL
PCOS
C Skeletal Muscle
p-AKT
β-Actin
CTRL
PCOS
p-AKT expression level
2.5
2.0
1.5
1.0
0.5
*
Ctrl
PCOS

Figure 7

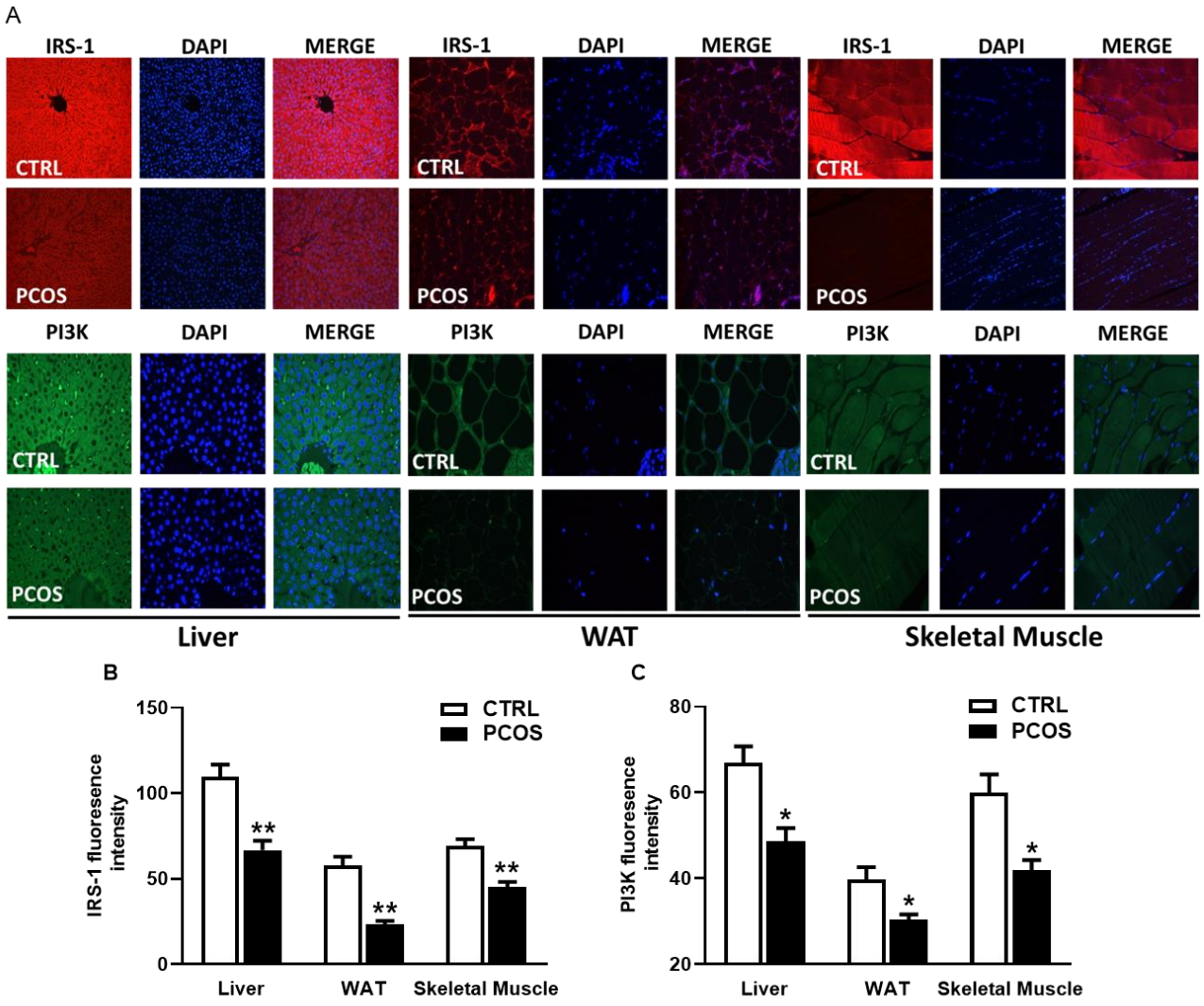
A
IRS-1
DAPI
MERGE
CTRL
PCOS
PI3K
Liver
WAT
Skeletal Muscle
B
IRS-1 fluoresence intensity
150
100
50
0
CTRL
PCOS
**
Liver
WAT
Skeletal Muscle
C
PI3K fluoresence intensity
80
60
40
20
*

Figure 8

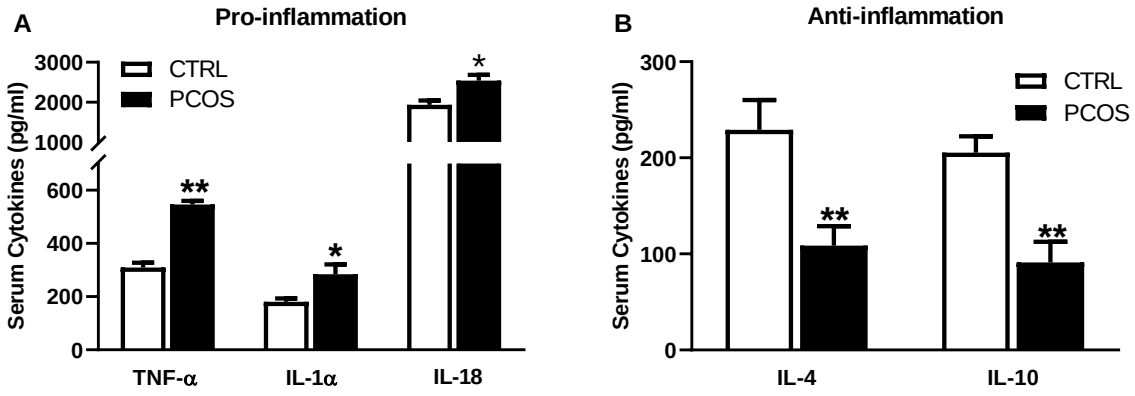

Figure 9

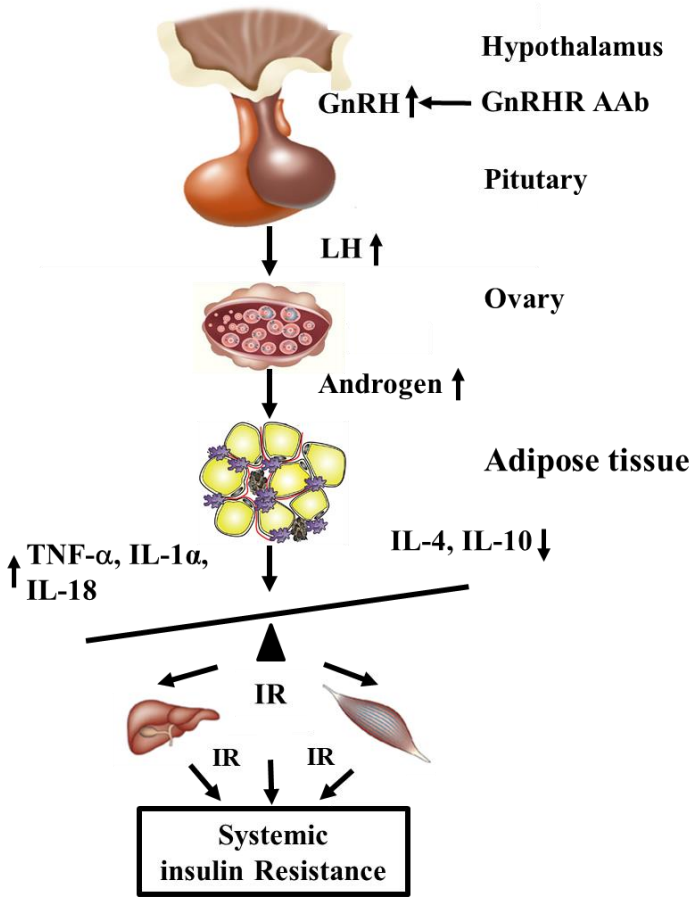

Table 1 Primers used in RT-PCR

Primer	Forward	Reverse
IR	GGCCCGATGCTGAGAACA	CGTCATTCCAAAGTCTCCGA
IRS-1	GATACCGATGGCTTCTCAGACG	TCGTTCTCATAATACTCCAGGCG
PI3K	AGATGCTTTCAAACGCTAT	GCTGTCGCTCACTCCA
AKT	CCTGAGGTGCTAGAGGACAAT	GCTGAGGAAGAACCGATGC
GLUT-2	CTGGGTCTGCAATTTCATCA	CGTAAGGCCCGAGGAAGT
GLUT4	GCACAGCCAGGACATTGTTG	CCCCCTCAGCAGCGAGTGA